BULLETIN OF THE POLISH ACADEMY OF SCIENCES
TECHNICAL SCIENCES, Vol. 63, No. 4, 2015
DOI: 10.1515/bpasts-2015-0113

Modelling and fault-tolerant control of 5-phase induction machine

M. ROLAK[1]*, H.S. CHE[2], and M. MALINOWSKI[3]

[1] Institute of Eletrical Machines, Warsaw University of Technology, 1 Politechniki Sq., 00-661 Warsaw, Poland
[2] UMPEDAC, University of Malaya, Jalan Lembah Pantai Baharu, 59990 Kuala Lumpur, Malaysia
[3] Institute of Control and Industrial Electronics, Warsaw University of Technology, 75 Koszykowa St., 00-662 Warsaw, Poland

Abstract. The paper presents modeling and analysis of a 5-phase induction machine connected to 2-level 5-leg converter in case of open-phase failure. A control of the machine is accomplished using the Field Oriented Control with hysteresis current controllers. Moreover, a fault-tolerant algorithm is addressed and simulated.

Key words: multiphase machine, fault-tolerant, post-fault, fault detection.

1. Introduction

A ubiquitous presence of induction motors throughout whole industry sector results in their utilization in many crucial high-reliability applications as well. However, even with multi-level converter topologies and more advanced control algorithms, the three-phase induction motors are unable to work properly under an open-phase fault condition, unless special converters [1] or connections are used [2]. This issue has an important impact on applications such an aircraft or off-shore wind generation systems [3]. In the first case, safety is the main consideration, such as mentioned in "more electric aircraft" [4]. In case of off-shore generators, fault will have profound economic impact as the generator can have a long downtime due to its remote location that prohibits fast repair. Different proposals for increasing reliability through a redundant converter or machine sets were proposed in [5], at the cost of taking up an extra space. This is why multiphase machines have attracted more and more attention of researchers recently [6]. Besides their inherent feature of being able to maintain rotating magnetic flux in case of phase fault, multiphase machines offer some additional advantages compared to their 3-phase counterparts. These include lower torque ripples and the higher power density coefficient and lower audible noise level [7]. It is important to notice that even if a multiphase machine can maintain rotating flux, it can be highly deformed what may cause large electromagnetic torque ripples and in turn, shorten bearings lifetime. Additionally, during phase fault, an unequal currents amplitudes lead to non-uniform heating of machine iron core and windings what significantly reduces windings lifetime. All mentioned issues demand a more in-depth investigation on various aspects of multiphase machines research, such as multilevel topologies [8], modulation techniques [9], fault-tolerant control [10,11], as well as phase-fault detection [12]. In the past, multiphase machines of different types, phase numbers and winding configurations have been reported [13]. In the paper, the modeling of a five-phase induction machine with single neutral point is developed, to fully describe the machine's behavior under both healthy and faulty conditions. Particularly, this paper presents method of phase lost modeling by calculation of back-EMF (instead of utilization of circuit breakers that allow for simulation of phase lost mainly in current zero-crossing condition). Although this approach was published previously in [14], neither the dynamic states nor fault-tolerant algorithm were presented. Several basic vector control methods for conventional three-phase induction machines have been developed in the last decades [15]. Not all of them have found wide industrial applications. Although the state space based approach is very promising method [16], the most popular strategy used commercially is Field Oriented Control (FOC). Finally, in this paper a post-fault FOC with hysteresis current controllers is presented and verified by simulation during transient post-fault states.

2. Modelling

2.1. Machine model. A basic approach to modelling a multiphase machine is described in [13] and similar notation is used in this paper. The basic equations that describe a squirrel cage induction machine are shown in (1). Here, several assumptions are made: the magnetic field is of sinusoidal distribution, parameters are temperature and time invariant and there is no saturation effect in the core.

$$\begin{aligned}
[v_s] &= [R_s]\cdot[i_s] + \frac{d}{dt}\left[[L_{ss}]\cdot[i_s] + [L_{sr}]\cdot[i_r]\right], \\
[v_r] &= [R_r]\cdot[i_r] + \frac{d}{dt}\left[[L_{rr}]\cdot[i_r] + [L_{rs}]\cdot[i_s]\right], \\
T_e &= \frac{P}{2}[i]^t \frac{d[L]}{d\theta_r}[i], \\
T_e - T_L &= J\frac{d\omega_{rm}}{dt} + c\cdot\omega_{rm},
\end{aligned} \tag{1}$$

*e-mail: michal.rolak@ee.pw.edu.pl

where v_s – stator phase voltages vector, v_r – rotor phase voltages vector (that in case of squirrel cage induction machine equals 0), i_s – stator phase currents vector, i_r – rotor phase currents vector, R_s – stator winding phase resistance matrix, R_r – rotor winding phase resistance matrix, L_{ss} – stator self and mutual inductance matrix, L_{rr} – rotor self and mutual inductance matrix, L_{sr} – stator to rotor mutual inductance matrix, L_{rs} – rotor to stator inductance matrix. Two last equations of (1) describe the electromechanical and mechanical dependencies where P – number of pole pairs, L – matrix of size 2×2 consisted of matrices L_{ss}, L_{sr}, L_{rs}, L_{rr}, respectively, see (6), T_e – electromechanical torque, T_L – load torque, ω_{rm} – mechanical angular speed, θ_r – rotor electrical angle, c – friction coefficient and J – inertia of rotating mass.

Despite the higher number of equations, the modelling procedure for a five-phase machine is similar to the method used in case of 3-phase machines. Equations (1) describe the machine model in phase a, b, c, d, e natural phase reference frame. However, it is possible to simplify the model analysis by transforming voltages, currents and fluxes denoted in general as g variables vector in (2)

$$[g_{\alpha\beta xy0}] = [T_5]\,[g_{abcde}] \tag{2}$$

into stationary (α, β, x, y, 0) reference frame utilizing transformation (3) which is also known as the decoupling matrix. The term *decoupling* is used because the resultant machine equations appear as multiple *decoupled planes*, with the variables corresponding to electromagnetic conversion being placed only in $\alpha-\beta$ plane, while the remaining loss-producing variables are located on $x-y$ planes. The angle utilized in the decoupling transformation is $\gamma = 2\pi/N$ where N is the phase number and equals 5.

$$[T_6] = \sqrt{\frac{2}{5}} \cdot \begin{bmatrix} 1 & \cos\gamma & \cos 2\gamma & \cos 3\gamma & \cos 4\gamma \\ 0 & \sin\gamma & \sin 2\gamma & \sin 3\gamma & \sin 4\gamma \\ 1 & \cos 2\gamma & \cos 4\gamma & \cos 6\gamma & \cos 8\gamma \\ 0 & \sin 2\gamma & \sin 4\gamma & \sin 6\gamma & \sin 8\gamma \\ \frac{1}{\sqrt{2}} & \frac{1}{\sqrt{2}} & \frac{1}{\sqrt{2}} & \frac{1}{\sqrt{2}} & \frac{1}{\sqrt{2}} \end{bmatrix}. \tag{3}$$

In [17] it is proved that these planes are orthogonal to each other what means that equations considered in one plane do not affect equations mapped into remaining ones. Moreover, harmonics of different orders are mapped onto different planes, as it is described in [18]. It should be mentioned here that the transformation (3) is in its power invariant form, where its inverse form can be easily obtained by simple transposition. In the case of a 5-phase induction machine, there are two complex planes which are denoted here as the $\alpha-\beta$, x_1-y_1 and one zero component. It can be noticed in [13] that the latter may be ignored when a single neutral point is used. This allows a multiphase machine to be analyzed in a way similar to a 3-phase machine what in turn, allows to utilize a similar control schemes. The transformed 5-phase induction machine can be expressed in terms of their stator and rotor equations, as (4) and (5) respectively

$$\begin{bmatrix} v_{s\alpha} \\ v_{s\beta} \\ v_{sx_1} \\ v_{sy_1} \\ v_{s0} \end{bmatrix} = [R_s] \begin{bmatrix} i_{s\alpha} \\ i_{s\beta} \\ i_{sx} \\ i_{sy} \\ i_{s0} \end{bmatrix} + \frac{d}{dt} \left(\begin{bmatrix} L_{ls}+M & 0 & 0 & 0 & 0 \\ 0 & L_{ls}+M & 0 & 0 & 0 \\ 0 & 0 & L_{ls} & 0 & 0 \\ 0 & 0 & 0 & L_{ls} & 0 \\ 0 & 0 & 0 & 0 & L_{ls} \end{bmatrix} \begin{bmatrix} i_{s\alpha} \\ i_{s\beta} \\ i_{sx} \\ i_{sy} \\ i_{s0} \end{bmatrix} + L_m \begin{bmatrix} c_{\theta_r} & -s_{\theta_r} & 0 & 0 & 0 \\ s_{\theta_r} & c_{\theta_r} & 0 & 0 & 0 \\ 0 & 0 & 0 & 0 & 0 \\ 0 & 0 & 0 & 0 & 0 \\ 0 & 0 & 0 & 0 & 0 \end{bmatrix} \begin{bmatrix} i_{r\alpha} \\ i_{r\beta} \\ i_{rx} \\ i_{ry} \\ i_{r0} \end{bmatrix} \right). \tag{4}$$

$$\begin{bmatrix} v_{r\alpha} \\ v_{r\beta} \\ v_{rx_1} \\ v_{ry_1} \\ v_{r0} \end{bmatrix} = [R_r] \begin{bmatrix} i_{r\alpha} \\ i_{r\beta} \\ i_{rx} \\ i_{ry} \\ i_{r0} \end{bmatrix} + \frac{d}{dt} \left(\begin{bmatrix} L_{lr}+M & 0 & 0 & 0 & 0 \\ 0 & L_{lr}+M & 0 & 0 & 0 \\ 0 & 0 & L_{lr} & 0 & 0 \\ 0 & 0 & 0 & L_{lr} & 0 \\ 0 & 0 & 0 & 0 & L_{lr} \end{bmatrix} \begin{bmatrix} i_{r\alpha} \\ i_{r\beta} \\ i_{rx} \\ i_{ry} \\ i_{r0} \end{bmatrix} + L_m \begin{bmatrix} c_{\theta_r} & s_{\theta_r} & 0 & 0 & 0 \\ -s_{\theta_r} & c_{\theta_r} & 0 & 0 & 0 \\ 0 & 0 & 0 & 0 & 0 \\ 0 & 0 & 0 & 0 & 0 \\ 0 & 0 & 0 & 0 & 0 \end{bmatrix} \begin{bmatrix} i_{s\alpha} \\ i_{s\beta} \\ i_{sx} \\ i_{sy} \\ i_{s0} \end{bmatrix} \right), \tag{5}$$

where L_{ls} – stator leakage inductance, L_{lr} – rotor leakage inductance, L_m – mutual inductance, $M = 2.5L_{mr}$, $c_{\theta_r} = 2.5\cos\theta_r$ and $s_{\theta_r} = 2.5\sin\theta_r$. As it was mentioned earlier L matrix of (1) consists of:

$$[L] = \begin{bmatrix} [L_{ss}] & [L_{sr}] \\ [L_{rs}] & [L_{rr}] \end{bmatrix}. \tag{6}$$

However, only matrices L_{sr} and L_{rs} are θ_r dependent. Hence, electromagnetic torque equation has a form as in (7).

$$\begin{aligned} T_e = PM\,[&\cos\theta_r\,(i_{s\beta}i_{r\alpha} - i_{s\alpha}i_{r\beta}) \\ &- \sin\theta_r\,(i_{r\alpha}i_{s\alpha} + i_{r\beta}i_{s\beta})] \end{aligned} \tag{7}$$

and indeed, utilizes only $\alpha-\beta$ variables as mentioned earlier. It is worth mentioning here that the rotor and stator currents and voltages are in their own reference frames.

2.2. Open-phase fault modeling. There are different approaches to model a faulted multiphase machine, such as presented in [19, 20]. In this paper the method based on back-EMF calculation presented in [14] is used for dynamic open phase-fault simulation which, in turn, allows to a clear depiction of the fault-tolerant algorithm application. Moreover, the dynamics issues of fault-tolerant control application may be crucial for high-reliability solutions. For purpose of discussion in this paper, the phase a is chosen arbitrarily as the phase with open-phase fault. Calculation of back-EMF bases on obtaining an induced voltage in faulted phase and its application into machine model input terminal. This can be calculated by utilizing Eqs. (2) and (3) with the phase current of the faulted phase being zero. The g variables in (2) can describe both currents and voltages quantities. When transforming variables from natural reference frame into stationary reference frame, the following dependencies can be observed:

$$g_\alpha - g_x = \sqrt{\frac{2}{5}}\,(g_b - g_c - g_d + g_e)\,(\cos\gamma - \cos 2\gamma)\,, \tag{8}$$

$$\begin{aligned} g_\alpha + g_x = 2\sqrt{\frac{2}{5}}g_a + \sqrt{\frac{2}{5}}\,&(g_b + g_c + g_d + g_e) \\ &\cdot(\cos\gamma + \cos 2\gamma)\,, \end{aligned} \tag{9}$$

when g_α is unknown, then 1st, 3rd and 5th equations of (2) are unknown as well when stator voltages are considered. However, when stator currents are considered and assuming that faulted phase current is 0, and that Kirchhoff's Current Law applied to (9) is still valid for star connected faulted machine, then substituting currents as a g variables it can be stated:

$$i_{s\alpha} + i_{sx} = 0 \implies i_{sx} = -i_{s\alpha}. \tag{10}$$

Furthermore Eq. (10) can be substituted into v_{sx} equation in (4) resulting in:

$$v_{sx} = -R_s i_{s\alpha} - \frac{d}{dt}L_{ls}i_{s\alpha}. \tag{11}$$

The Eq. (11) can be substituted into stator voltage equation expressed by (8):

$$\begin{aligned} v_{s\alpha} = \sqrt{\frac{2}{5}}\,&(v_{sb} - v_{sc} - v_{sd} + v_{se})\,(\cos\gamma - \cos 2\gamma) \\ &- R_s i_{s\alpha} - \frac{d}{dt}L_{ls}i_{s\alpha}. \end{aligned} \tag{12}$$

Finally, the Eq. (12) is substituted into Eqs. (2) and (3). As a result of this operation, it is possible to calculate induced back-EMF in the phase a:

$$\begin{aligned} v_{s\alpha} = &-(v_{sb} + v_{se})\cos 2\gamma - (v_{sc} + v_{sd})\cos\gamma \\ &-\sqrt{\frac{5}{2}}\left(R_s i_{s\alpha} + \frac{d}{dt}L_{ls}i_{s\alpha}\right). \end{aligned} \tag{13}$$

3. Control

3.1. Healthy condition. Due to greatly simplified analysis by applying (2), the well-known control strategy such FOC can be applied directly on 5-phase machine. Figure 1 presents the FOC scheme for 5-phase induction machine working in healthy mode. It can be noticed that $i_{d'}$ and i_q component corresponds to rotor flux and torque producing currents, respectively. The coordinate transformation sequence is exactly the same as for 3-phase machine. It is worth noting that in rotating $d'-q$ reference coordinates for 5-phase machine the d component suffix is enriched with apostrophe to differentiate it against the phase d suffix. Remaining references i.e. x_1, y_1, and the zero sequence are set to 0. Naturally, a proper rotor flux angle is required which is calculated as an integral of two signals sum i.e: the rotor's electrical speed and the speed controller output multiplied by a Slip Gain (SG_n) coefficient which is described by Eq. (14):

$$SG = \frac{i_q^*}{\tau_r i_{d'}^*}, \tag{14}$$

where $\tau = (L_{lr} + L_m)/R_r$. Usually, the calculated $d'-q$ values are inputs for modulator such a SVM or Sine-PWM in many modern 3-phase solutions [21]. However, here in this paper a hysteresis current controller is addressed. Despite of the variable switching frequency, hysteresis controller has the advantages of being simple, fast, and allows for implementation of the fault-tolerant control without the need of additional PI controllers such as in [10, 19].

Note that the proper transformation (15) of converter pole voltages has to be made when a power converter is utilized in simulation model. It has to be done, because the machine utilizes phase voltages on its inputs.

$$v_k = V_k - \frac{1}{5}(V_a + V_b + V_c + V_d + V_e), \tag{15}$$

where $k = \{a, b, c, d, e\}$ and V – describes particular leg pole voltage.

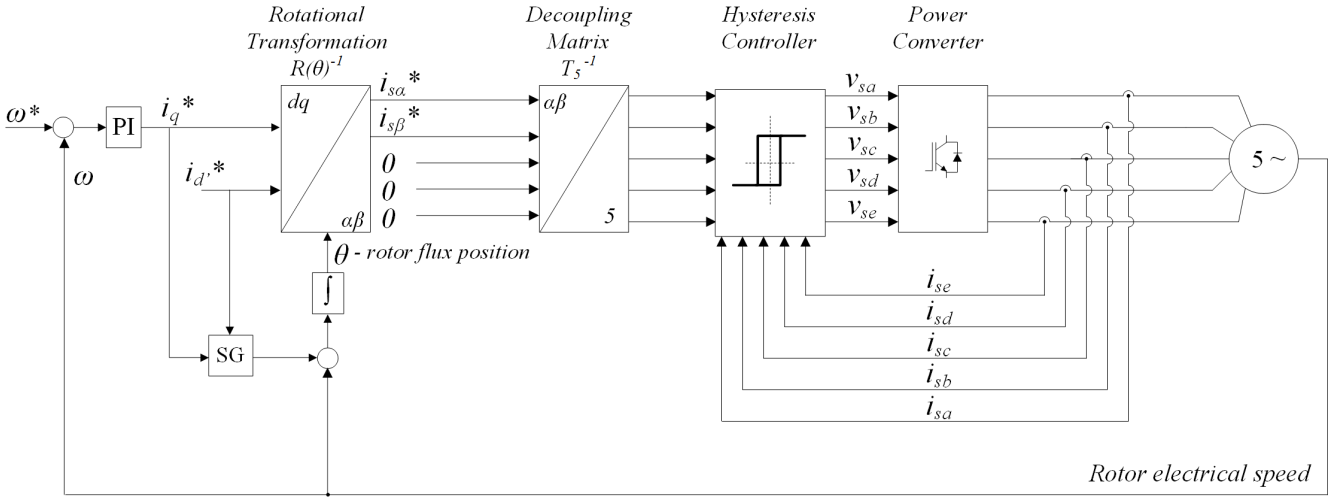

Fig. 1. Indirect Rotor Field Oriented Control scheme with hysteresis current controllers

3.2. Open-phase fault. Due to the fact that faulted model utilizes the same transformation matrix (3) as the healthy one, it is possible to modify the control algorithm and adopt it to the post-fault condition. It should be stressed that the model of faulted machine does not change, except that the current in faulted phase is zero, and due to this reason only transformed values of currents are changed similarly to (8), (9) according to (2). In order to maintain a smooth post-fault operation, it is important to maintain a smooth rotating magnetic flux. This is achieved by solving machine equations to finding current references that give a circular current trajectory on the $\alpha - \beta$ plane. It is necessary to calculate $x_1 - y_1$ current components which can compensate for the distorted $\alpha - \beta$ current components. This can be solved in different ways such as in [22], where new post-fault current references are required. The other method of fault-tolerant approach bases on modified (3) transformation and is described in [20].

3.3. Fault-tolerance. New fault-tolerant currents references that forms magnetic flux vector circular trajectory can be obtained by solving Eq. (16) with $i_{sa} = 0$ in similar manner as presented for six-phase machine in [19]:

$$\begin{bmatrix} i_{sa} \\ i_{sb} \\ i_{sc} \\ i_{sd} \\ i_{se} \end{bmatrix} = \begin{bmatrix} 1 & 0 & 1 & 0 & \frac{1}{\sqrt{2}} \\ \cos\gamma & \sin\gamma & \cos 2\gamma & \sin 2\gamma & \frac{1}{\sqrt{2}} \\ \cos 2\gamma & \sin 2\gamma & \cos 4\gamma & \sin 4\gamma & \frac{1}{\sqrt{2}} \\ \cos 3\gamma & \sin 3\gamma & \cos 6\gamma & \sin 6\gamma & \frac{1}{\sqrt{2}} \\ \cos 4\gamma & \sin 4\gamma & \cos 8\gamma & \sin 8\gamma & \frac{1}{\sqrt{2}} \end{bmatrix} \begin{bmatrix} i_{s\alpha} \\ i_{s\beta} \\ i_{sx} \\ i_{sy} \\ i_{s0} \end{bmatrix}. \tag{16}$$

For the five-phase machine with the star-connected neutral point, the zero-sequence current can be ignored and this reduces the number of equations to be solved. In order to maintain a circular rotating magnetic flux in post-fault condition, the $\alpha - \beta$ currents should be in the following form:

$$\begin{aligned} i_{s\alpha} &= |I_{s\alpha}| \cos\theta_r, \\ i_{s\beta} &= |I_{s\beta}| \cos\theta_r. \end{aligned} \tag{17}$$

Then i_{sx} and i_{sy} current components can be used to generate proper set of stator phase currents. This can be achieved by making them dependent on $i_{s\alpha}$ and $i_{s\alpha}$ as presented in (18):

$$\begin{aligned} i_{sx} &= K_1 i_{s\alpha} + K_2 i_{s\beta}, \\ i_{sy} &= K_3 i_{s\alpha} + K_4 i_{s\beta}. \end{aligned} \tag{18}$$

Then (17), (18) can be substituted into (16), and unknown coefficients K_{1-4} can be calculated off-line to meet given restrictions, e.g. to have equal stator currents amplitudes. The idea of fault-tolerant control method is depicted in Fig. 2, and it clearly shows that only slight modification of control scheme presented in Fig. 1 is required.

Since a hysteresis controller is being utilized, it is not necessary to perform $\alpha - \beta$, $x_1 - y_1$ post-fault current analysis conducted in [19] which allows for reduction of current controllers. The solution of (18) is not unique and therefore there are different K_{1-4} coefficients that produce different current sets that can form circularly rotating magnetic flux vector. This is why some additional constrains can be declared for fault-tolerant strategies. This feature of post-fault system is presented in Fig. 3, where same hodographs of magnetic flux obtained from four different remaining stator phase currents are presented. Figure 3a presents K_{1-4} coefficients obtained without any additional constrains, whereas Fig. 3b was limited for the same amplitude in each phase for uniform windings heating.

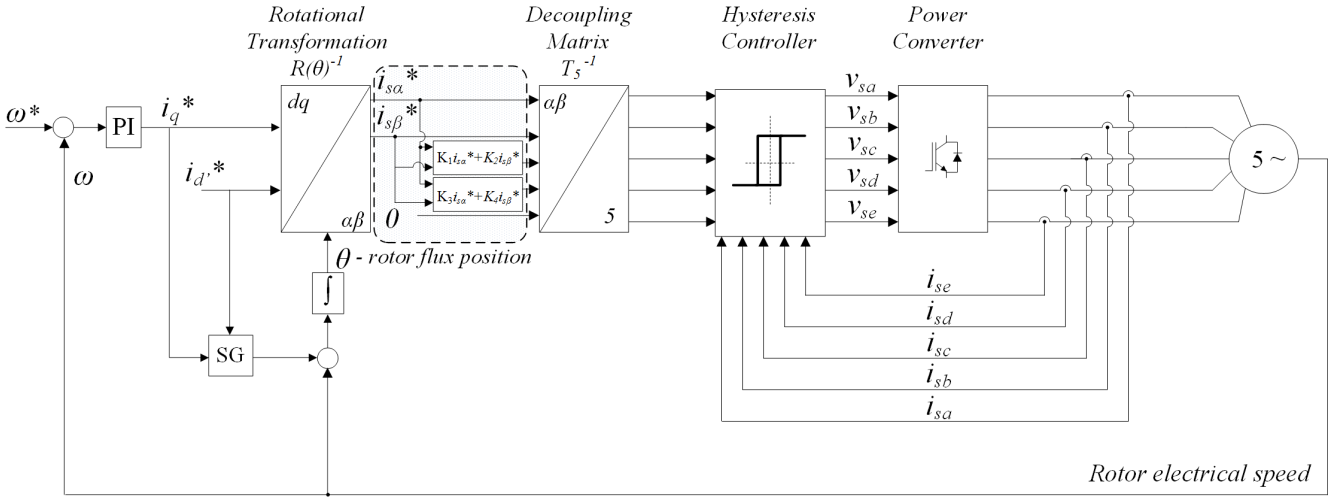

Fig. 2. Fault-tolerant FOC algorithm

a)

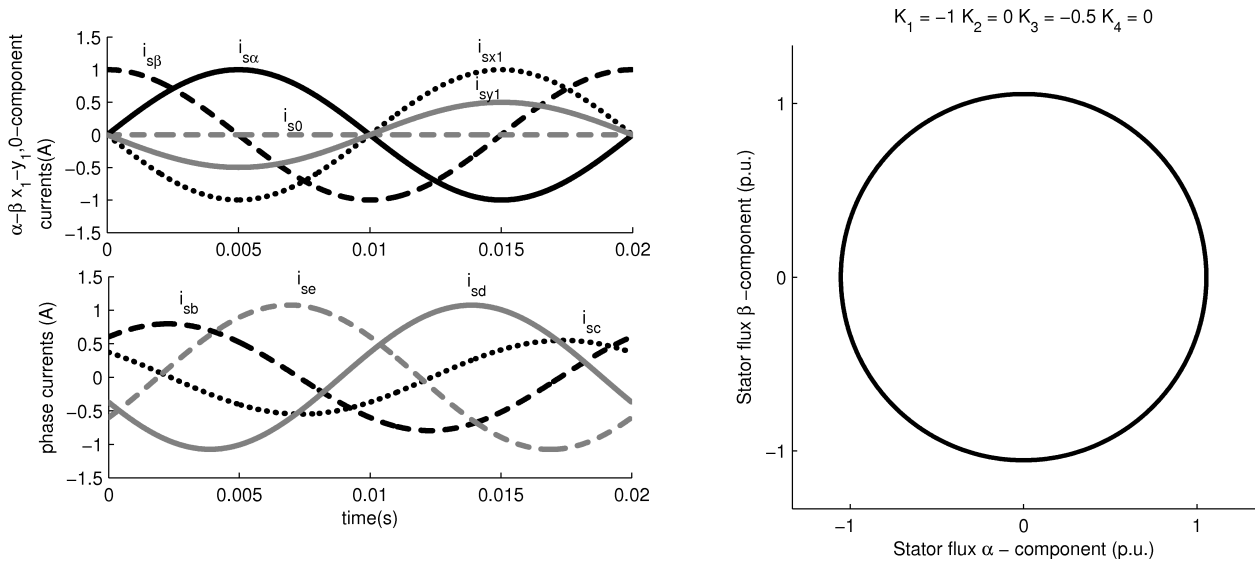

b)

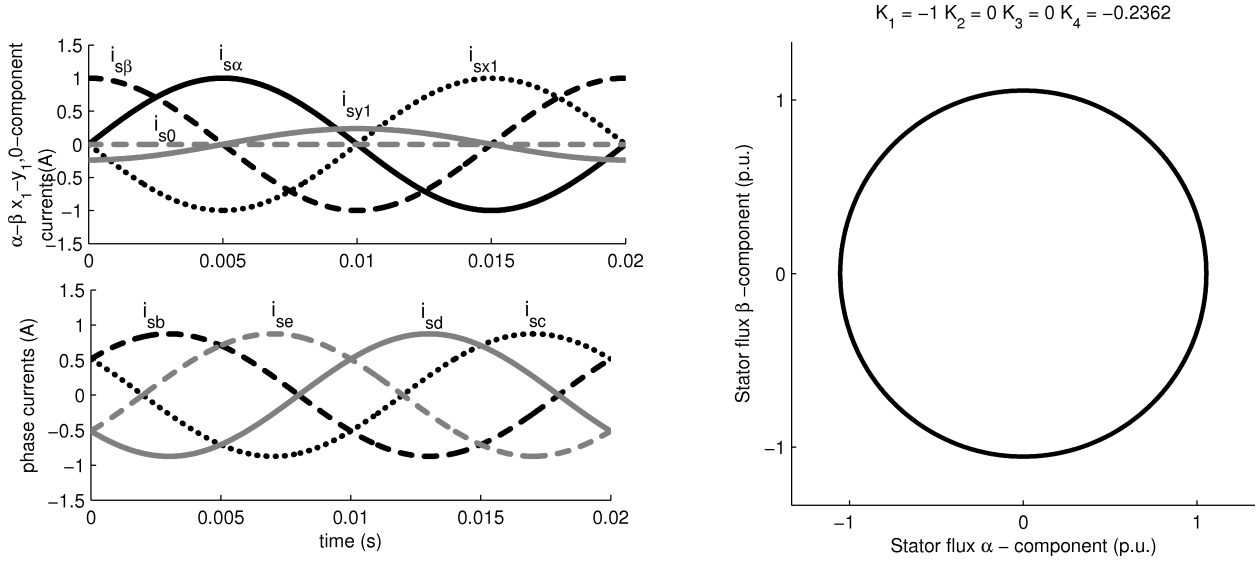

Fig. 3. Different K_x coefficient that fulfill circular trajectory of stator magnetic flux a) coefficients set $[K_1 = -1, K_2 = 0, K_3 = -0.5, K_4 = 0]$, b) coefficients set $[K_1 = -1, K_2 = 0, K_3 = 0, K_4 = -0.2362]$

4. Simulation results

In this section the characteristics for healthy and open-phase faulted 5-phase induction machine are presented. Moreover, simulation results of the FOC scheme for healthy, post-fault and fault-tolerant cases are addressed as well. As a simulation model of the star-connected, 5-phase symmetrical induction machine connected to 5-leg 2-level converter with fault in a phase was utilized and built in Matlab/Simulink simulation software. The machine model was built as a set of differential equations and the SimPowerSystem power electronics blocks were utilized to model power converters and passive components. Necessary data used in simulation are presented in Table I and these machine parameters mainly come from [23].

Table 1
Model parameters

Rated power	P_{rated}	3.6 kW
Stator leakage inductance	L_{ls}	49 mH
Rotor leakage inductance	L_{lr}	27 mH
Magnetizing inductance	L_m	526 mH
Stator resistance	R_s	2.5 Ω
Rotor resistance	R_r	1.7 Ω
Rotor inertia	J	0.03
Friction coefficient	c	0.0029

A first validation of addressed approach is to test induction machine of healthy and faulted model connected to fictional 5-phase grid. With running motor and gradually increasing load torque it is possible to find mechanical characteristics for both healthy and open-phased machines what is presented in Fig. 4a and Fig. 4b, respectively.

As it was mentioned, the faulted multiphase machine is able to work, however the increased torque ripples are generated. These ripples were removed with moving averaged filter in Fig. 4b for sake of clarity. It can be noticed that averaged rated power of faulted machine P'_{rated} is about 15% lower in comparison to healthy one. This clearly shows the inherent ability of multiphase machine to maintain its performance in case of at least one phase lost. Therefore, it is rather obvious that more advanced control strategies than constant Volt per Hertz control (V/f = const) have to be applied to fully utilize multiphase machine fault-tolerant features.

Thus, Fig. 5 presents the FOC algorithm working in three modes: healthy, post-fault and fault-tolerant, respectively. The set of K_x coefficients presented in Fig. 3a was utilized in this particular case.

The electromagnetic torque response can be observed in $t_0 = 1.5$ s after rotor flux is established. The reference frequency of simulations presented in Fig. 5 was 45 Hz, and test load of 5 Nm. A closer look of the rotor speed is also presented to show speed ripples as well. At $t_1 = 1.75$ s, the open-phase fault is applied and it is followed by operation of the fault-tolerant algorithm at $t_2 = 2.0$ s. The bottom-most waveform of Fig. 5 presents the stator currents where faulted phase a, denoted in solid black line, can be seen to reach 0 value after transient state. It can be observed that after t_1 some torque pulsations appear as a result of deformed stator currents. It can be mentioned that these ripples have higher amplitude than similar response presented in [24] where Sine-PWM modulation was applied and what in turn, can be considered as a drawback of chosen hysteresis current control. Additionally, it can be noticed that once fault-tolerant algorithm is applied, the stator current amplitudes increase in comparison to healthy condition what is necessary to maintain the same, ripple-free torque with the decreased number of phases. Figures 6 and 7 present flux vectors trajectories and currents in particular time spans with K_x coefficients obtained in Fig. 3a $[K_1 = -1, K_2 = 0, K_3 = -0.5, K_4 = 0]$. The same simulation was carried out with second set of K_x coefficients as shown in Fig. 3b $[K_1 = -1, K_2 = 0, K_3 = 0, K_4 = -0.2362]$.

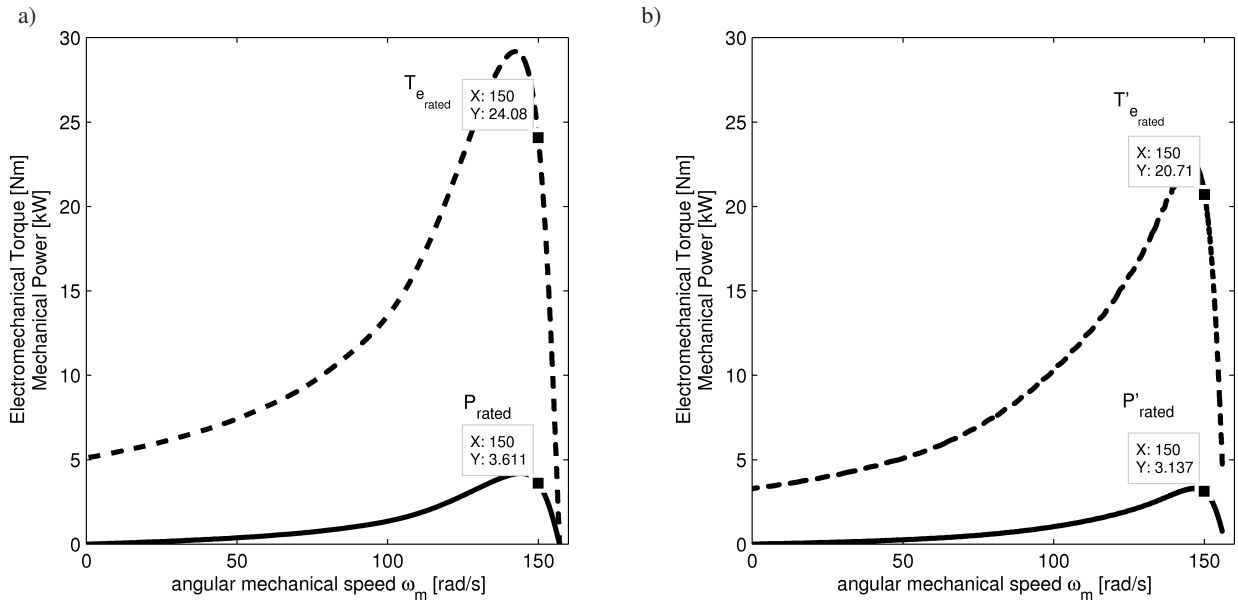

Fig. 4. a) 5-phase induction machine characteristics a) healthy condition, b) a-phase open-phase fault condition

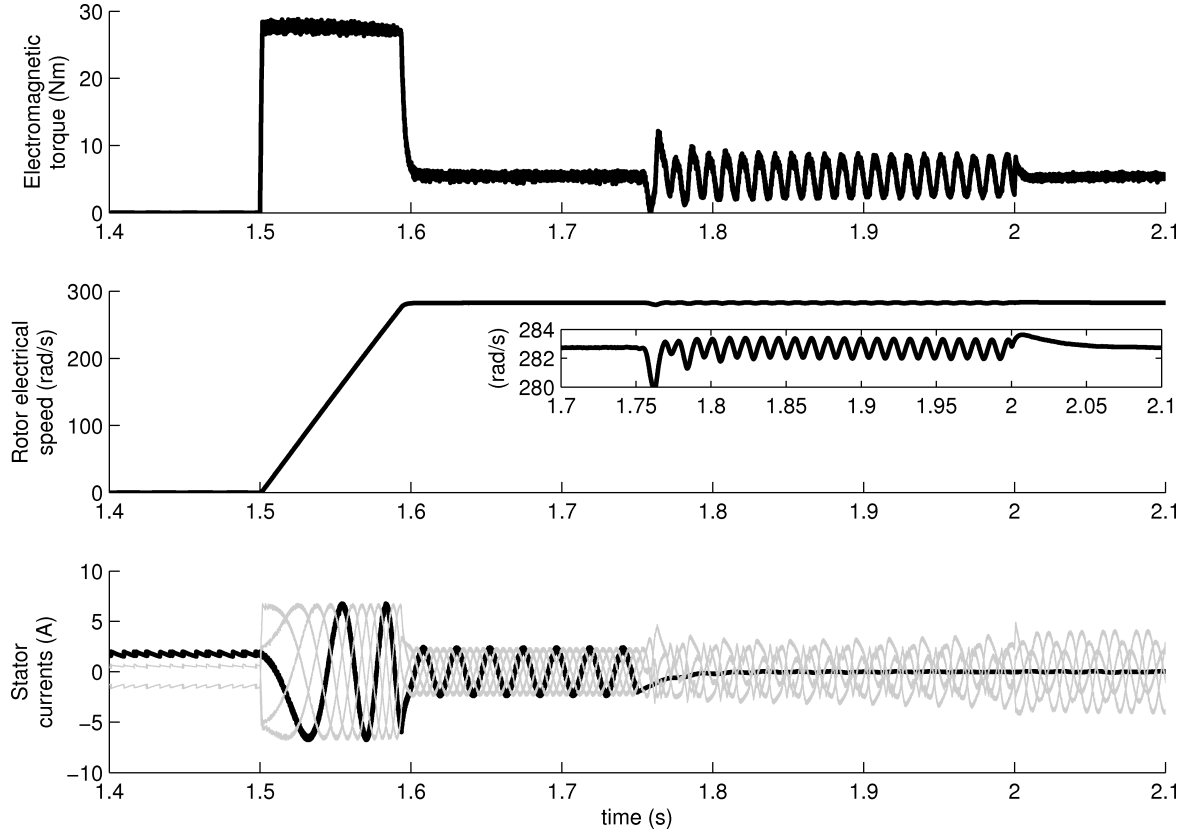

Fig. 5. Simulation of start-up and operation at 45 Hz for FOC during healthy, post-fault and fault-tolerant condition

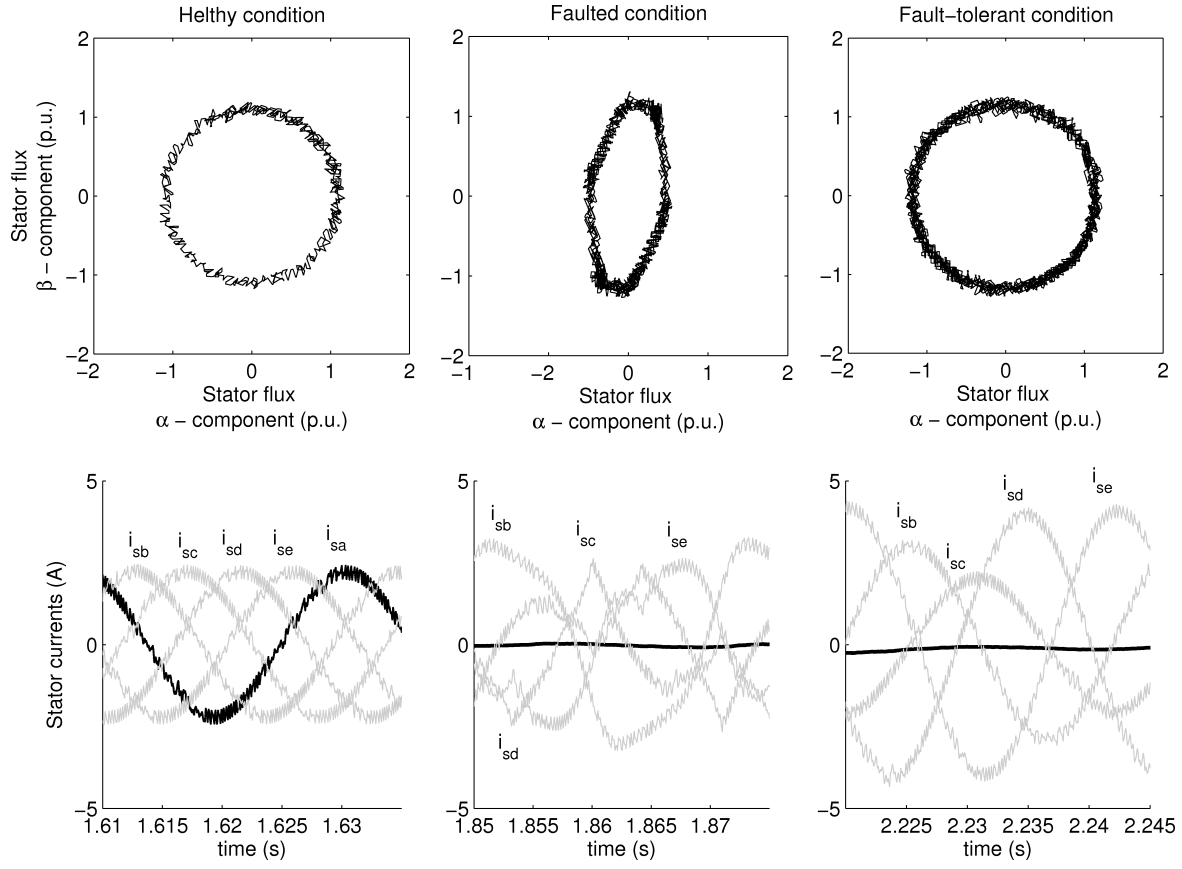

Fig. 6. Hodographs and current waveforms for particular cases a) healthy, b) post-fault, c) fault-tolerant (K-coefficients as in Fig. 3a)

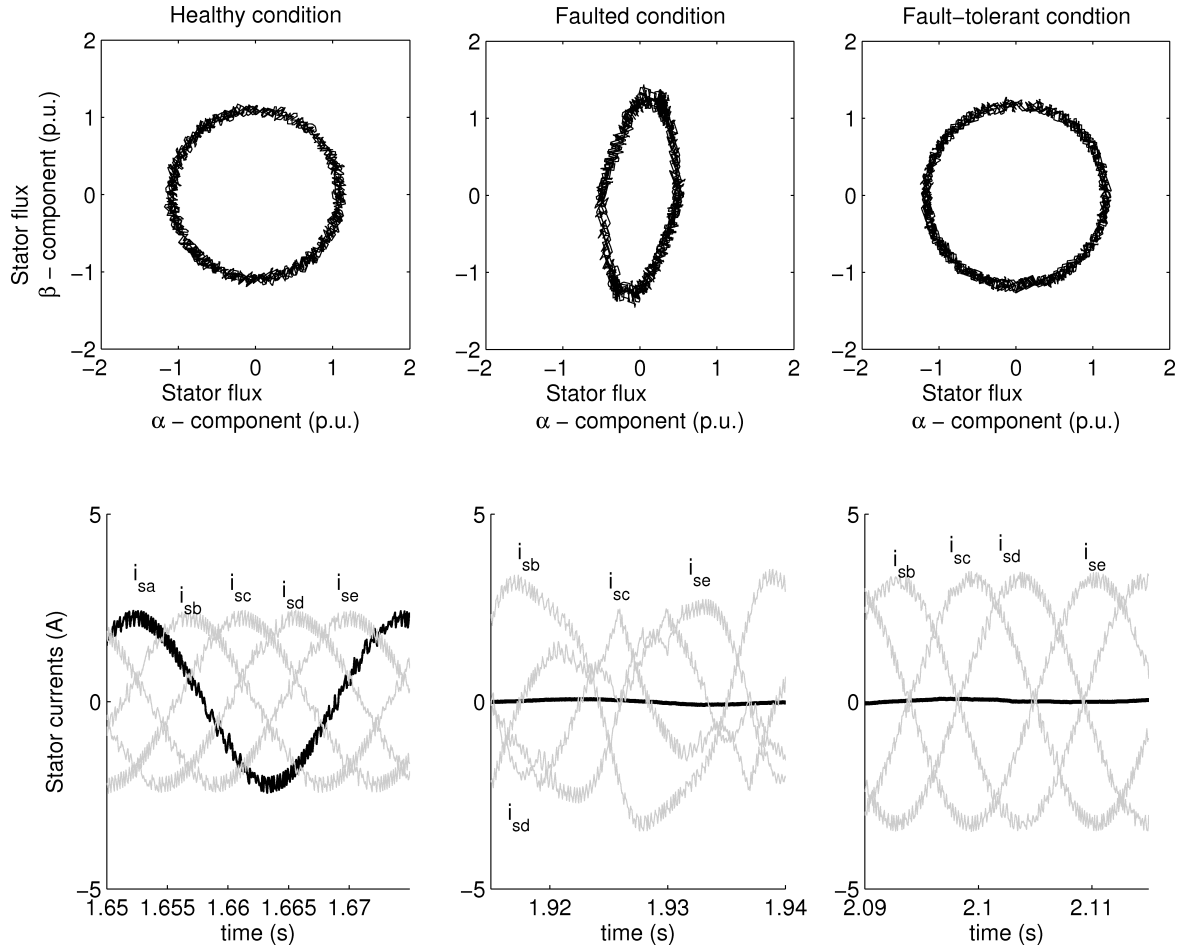

Fig. 7. Hodographs and current waveforms for particular cases a) healthy, b) post-fault, c) fault-tolerant (K-coefficients as in Fig. 3b)

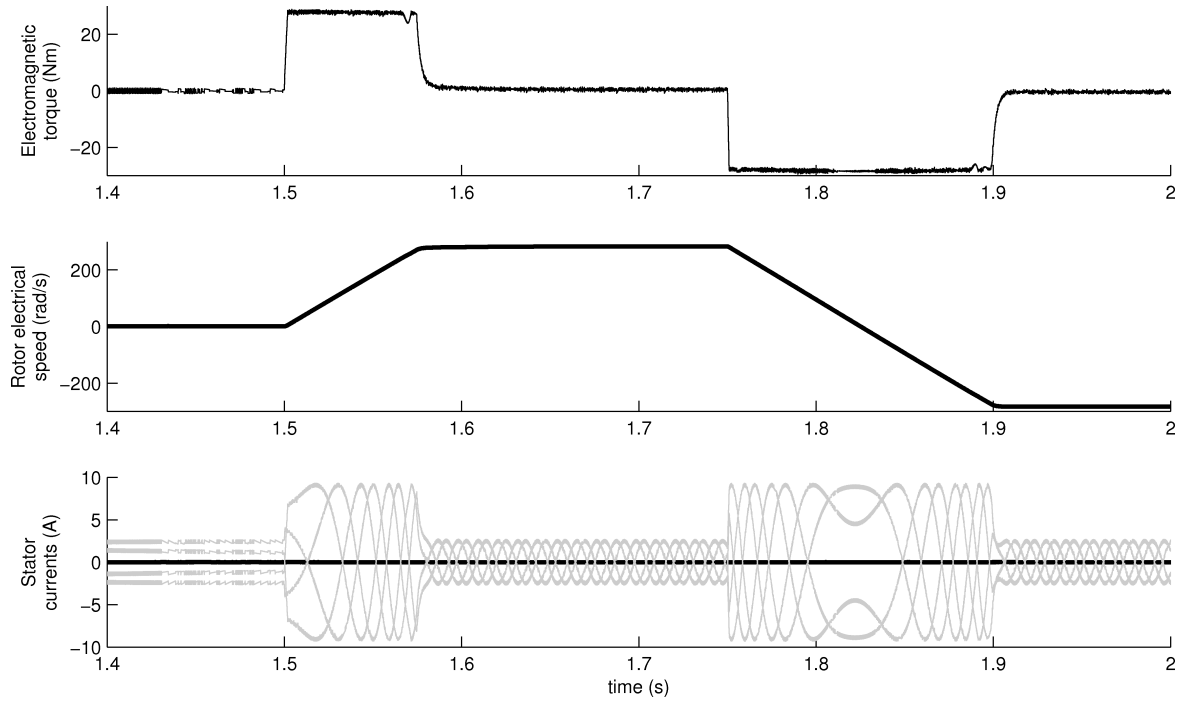

Fig. 8. Machine start-up with fault-tolerant algorithm under load condition

The post-fault algorithm allows the 5-phase induction machine to operate without one phase even in start-up conditions which is impossible in case of 3-phase machine. This case is presented in Fig. 8 together with speed reversal as well. The K_x coefficients presented in Fig. 3b was applied this time due to equal currents amplitudes.

Note that the presented simulations do not assume power de-rating, which should be considered in a practical application mainly due to risk of overheating and exceeding winding rated currents. On the other hand, it is also possible to design machine with winding ratings that can withstand larger currents magnitudes. In that case, full machine power can still be obtained even after open-phase fault.

5. Conclusions

In this paper, simulation models for healthy and faulty 5-phase induction machine with one open-phase were shown and analysed. The chosen method for fault modelling utilizing back-EMF allows for analysis of dynamic transient states during healthy, post-fault and fault-tolerant operation modes. Additionally, a comparison of healthy and faulted induction machine characteristics are presented and briefly analyzed. A proposal of simple fault-tolerant FOC with hysteresis current controller was presented and simulated. However, the presented solution has some disadvantages such as the necessity of performing off-line calculation of fault-tolerant K_x coefficients. Nonetheless, the presented approach allows for further analysis of post-fault transient states which is especially important in case of fault detection algorithms.

Acknowledgements. This work was supported by a scholarship for Ph.D. students founded by the Center of Advanced Studies at the Warsaw University of Technology in the Program CAS/24/POKL.

REFERENCES

[1] M. Rottach, C. Gerada, and P.W. Wheeler, "Evaluation of motor-drive segmentation strategies for fault-tolerance", *2013 IEEE ECCE Asia Downunder* 1, 530–536 (2013).

[2] T-H. Liu, J-R. Fu, and T.A. Lipo, "A strategy for improving reliability of field-oriented controlled induction motor drives", *Ind. Appl. IEEE Trans.* 29 (5), 910–918 (1993).

[3] J. Ribrant and L. Bertling, "Survey of failures in wind power systems with focus on Swedish wind power plants during 1997–2005", *Power Engineering Society General Meeting* 1, 1–8 (2007).

[4] X. Roboam, B. Sareni, and A.D. Andrade, "More electricity in the air: toward optimized electrical networks embedded in more-electrical aircraft", *Ind. Electron. Mag. IEEE* 6 (4), 6–17 (2012).

[5] H. Burzanowska, P. Sario, C. Stulz, and P. Joerg, "Redundant Drive with Direct Torque Control (DTC) and Dual-Star Synchronous Machine, simulations and verification", *Power Electr. and Application, Eur. Conf.* 1, 1–10 (2007).

[6] E. Levi, R. Bojoi, F. Profumo, H.A. Toliyat, and S. Williamson, "Multiphase induction motor drives – a technology status review", *Electr. Power Appl. IET* 1 (4), 489–516 (2007).

[7] S.V. Ignatenko and A.N. Golubev, "Influence of number of stator-winding phases on the noise characteristics of an asynchronous motor", *Russ. Electr. Eng.* 71, 41–46 (2000).

[8] O. Dordevic, M. Jones, and E. Levi, "A comparison of carrier-based and space vector PWM techniques for three-level five-phase voltage source inverters", *Ind. Informatics, IEEE Trans.* 9 (2), 609–619 (2013).

[9] O. Lopez, J. Alvarez, F.D. Freijedo, A.G. Yepes, J. Malvar, P. Fernandez-Comesana, J. Doval-Gandoy, A. Nogueiras, A. Lago, and C.M. Penalver, "Multilevel multiphase space vector PWM algorithm with switching state redundancy applied to three-phase four-leg converters", *IECON 2010 – 36th Annual Conf. on IEEE Industrial Electronics Society* 1, 568–575 (2010).

[10] A. Tani, M. Mengoni, L. Zarri, G. Serra, and D. Casadei, "Control of multiphase induction motors with an odd number of phases under open-circuit phase faults", *Power Electron. IEEE Trans.* 27 (2), 565–577 (2012).

[11] P. Lezana, J. Pou, T.A. Meynard, J. Rodriguez, S. Member, S. Ceballos, S. Member, and F. Richardeau, "Survey on fault operation on multilevel inverters", *Power Electron. IEEE Trans.* 57 (7), 2207–2218 (2010).

[12] M. Salehifar, R.S. Arashloo, J.M. Moreno-Equilaz, V. Sala, and L. Romeral, "Fault detection and fault tolerant operation of a five phase PM motor drive using adaptive model identification approach", *Emerg. Sel. Top. Power Electron. IEEE* 2 (2), 212–223 (2014).

[13] E. Levi, "Multiphase AC machines: Chapter 3", in *The Industrial Electronics Handbook: Power Electronics and Motor Drives*, CRC Press, London, 2011.

[14] S. Karugaba, G. Wang, O. Ojo, and M. Omoigui, "Dynamic and steady-state operation of a five phase induction machine with an open stator phase", *Power Symp., 2008. NAPS '08. 40th North American* 1, 1–8 (2008).

[15] D. Stando and M.P. Kazmierkowski, "Simple speed sensorless DTC-SVM scheme for induction motor drives", *Compat. Power Electron. (CPE), 2013 8th Int. Conf.* 61 (2), 301–307 (2013).

[16] T. Tarczewski, L.M. Grzesiak, A. Wawrzak, K. Karwowski, and K. Erwinski, "A state-space approach for control of NPC type 3-level sine wave inverter used in FOC PMSM drive", *Bull. Pol. Ac.: Tech.* 62 (3), 439–448 (2014).

[17] Y. Zhao and T.A. Lipo, "Space vector PWM control of dual three-phase induction machine using vector space decomposition", *Ind. Appl. IEEE Trans.* 31 (5), 1100–1109 (1995).

[18] J. Malvar, A.G. Yepes, A. Vidal, P. Fernandez-Comesana, F.D. Freijedo, O. Lopez, and J. Doval-Gandoy, "Harmonic subspace and sequence mapping in a series-connected six-phase two-motor drive", *IECON 2012 – 38th Annual Conf. on IEEE Industrial Electronics Society* 1, 3622–3627 (2012).

[19] H.S. Che, M. Duran, E. Levi, M. Jones, W.P. Hew, and N.A. Rahim, "Post-fault operation of an asymmetrical six-phase induction machine with single and two isolated neutral points", *Energy Conversion Congress and Exposition (ECCE), 2013 IEEE* 1, 1131–1138 (2013).

[20] R. Kianinezhad, B. Nahid-Mobarakeh, L. Baghli, F. Betin, and G-A. Capolino, "Modeling and control of six-phase symmetrical induction machine under fault condition due to open phases", *IEEE Trans. Ind. Electron.* 55 (5), 1966–1977 (2008).

[21] D. Dujic, "Development of pulse-width-modulation techniques for multi-phse and multi-leg voltage source inverter", *PhD Thesis*, Liverpool John Moores University, Liverpool, 2008.

[22] J-R. Fu and T.A. Lipo, "Disturbance free operation of a multiphase current regulated motor drive with an opened phase", *Conf. Record 1993 IEEE Industry Applications Conf. Twenty-Eighth IAS Annual Meeting* 1, 637–644 (1993).

[23] J.A. Riveros, A.G. Yepes, F. Barrero, J. Doval-Gandoy, B. Bogado, O. Lopez, M. Jones, and E. Levi, "Parameter identification of multiphase induction machines with distributed windings; Part 2: time-domain techniques", *Energy Conversion, IEEE Trans.* 27 (4), 1067–1077 (2012).

[24] M. Rolak and M. Malinowski, "Six-phase symmetrical induction machine under fault states-modelling, simulation and experimental results", *Przeglad Elektrotechniczny* 90 (11), 91–95 (2014).